

Adaptive Cancellation of a Sinusoidal Disturbance with Rapidly Varying Frequency Using an Augmented Error Algorithm

Xiuyan Guo and Marc Bodson

Abstract—This paper considers a compensator for a sinusoidal disturbance with known but rapidly varying frequency. The compensator is obtained as an adaptive feedforward cancellation algorithm using an augmented error. The system is shown to be Lyapunov stable and equivalent to a linear time-varying controller that includes an internal model of the disturbance. The stability and robustness properties of the augmented error algorithm are validated by simulation results.

I. INTRODUCTION

We consider the problem of rejecting a sinusoidal disturbance whose frequency is known, but varies significantly over time. For example, [11] describes the problem of compensating periodic tension disturbances in web transport systems. Experiments on testbed showed that the spectrum of the web tension had large components at the frequencies of rotation of the winding and unwinding rolls, due to the eccentricity and the non-circularity of the rolls. Fig. 1 shows the frequencies of the sinusoidal disturbance components. The fundamental frequency f_1 associated with the unwinding roll increases with time, in relation to the decreasing radius, and the frequency f_2 associated with the winding roll similarly decreases over time. In [10], an adaptive

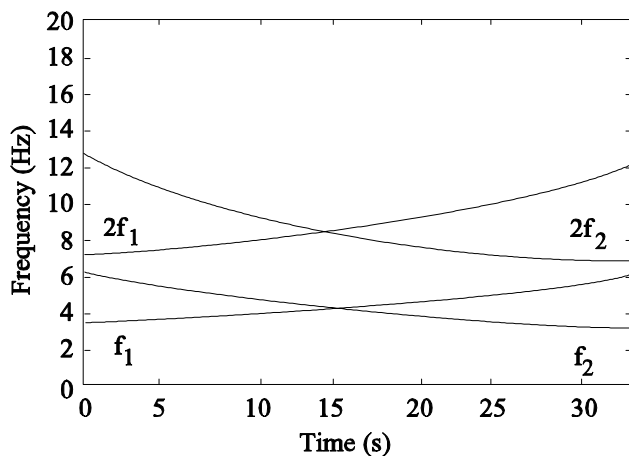


Fig. 1. Frequencies of the disturbance components in the web tension

compensation method was proposed to reject a sinusoidal disturbance with time-varying frequency, due to eccentricity

This work was supported by the National Science Foundation under Grant No. ECS0115070.

The authors are with the Department of Electrical and Computer Engineering, University of Utah, 50 S Central Campus Dr Rm 3280, Salt Lake City, UT 84112, USA.

in mechanical systems. In both applications, the frequencies of the disturbances could be obtained using tachometers on the motors, or by differentiating angular position signals provided by encoders.

For periodic disturbance rejection with known frequency, the *internal model principle* (IMP) [1] [5] [7] is widely applied, and consists in incorporating a model of the dynamics of the disturbance signal in the compensator. In [3], output regulation was achieved by the cascade of two compensators. It was shown that the IMP compensator could be obtained in two steps: (a) creating an internal model in the forward path and (b) stabilizing the system. Note that if the frequency of the sinusoidal disturbance varies rapidly, the internal model becomes time-varying. The stabilizing compensator is then more difficult to design.

Several algorithms are available to solve the above problem. Because the frequency parameter appears linearly in an appropriate disturbance model, [6] proposed a *linear parameter-varying* (LPV) technique for the rejection of a sinusoidal disturbance with time-varying frequency. The *linear matrix inequality* (LMI) synthesis method was used to design controllers such that the closed-loop system was internally stable. Recently, [4] proposed disturbance cancellation designs based on gradient or pseudo-gradient algorithms. This paper extends the approach in [4] to exploit the benefits of an *augmented error* (AE) [8]. An advantage of the AE algorithm is that it can easily be designed to be stable, provided that the plant is known and stable.

The paper is organized as follows. Section II presents the adaptive feedforward cancellation scheme with AE algorithm. An appropriate model for the sinusoidal disturbance with varying frequency is provided in section III. In section IV, the adaptive algorithm with AE is shown to be equivalent to an IMP algorithm. In section V, the performance and robustness of the proposed algorithm are verified through some simulations.

II. ADAPTIVE FEEDFORWARD CANCELLATION ALGORITHM WITH AUGMENTED ERROR

An *adaptive feedforward cancellation* (AFC) scheme is shown in Fig. 2, where a *linear time-invariant* (LTI) plant $P(s)$ is perturbed by a sinusoidal disturbance of the form

$$\begin{aligned} d(t) &= \theta_c^* \cos(\alpha_d(t)) + \theta_s^* \sin(\alpha_d(t)) \\ \dot{\alpha}_d(t) &= \omega_d(t) \end{aligned} \quad (1)$$

The disturbance frequency $\omega_d(t)$ is assumed to be bounded and known. The control input $u(t)$ is chosen to be

$$u(t) = \theta_c(t) \cos(\alpha_d(t)) + \theta_s(t) \sin(\alpha_d(t)) \quad (2)$$

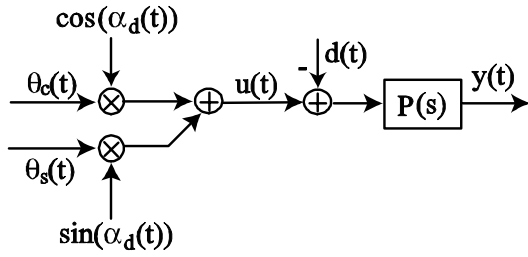


Fig. 2. Adaptive feedforward cancellation scheme

where $\theta_c(t)$ and $\theta_s(t)$ are adaptive parameters and θ_c^* and θ_s^* are nominal parameters. The nominal parameters are assumed to be constant, despite the frequency variation. This assumption reflects a category of problems associated with eccentricity compensation. For example, Fig. 3 shows an elliptical roll whose angular position is determined by $\alpha_d(t)$ and whose height is $d(t)$. Even when the frequency of rotation varies, $d(t)$ is a signal of the form (1) with constant coefficients θ_c^* , θ_s^* .

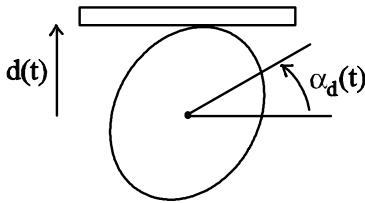


Fig. 3. Periodic disturbance associated with eccentricity

Exact disturbance cancellation can, in theory, be achieved by letting $\theta_c(t) = \theta_c^*$, $\theta_s(t) = \theta_s^*$. Since the nominal parameters are unknown, the control strategy is to use adaptive algorithms to adjust the parameters so that they converge to their nominal values. Let the nominal and adaptive parameter vectors be

$$\theta^* = \begin{pmatrix} \theta_c^* \\ \theta_s^* \end{pmatrix} \quad \theta(t) = \begin{pmatrix} \theta_c(t) \\ \theta_s(t) \end{pmatrix} \quad (3)$$

The regressor vector is defined to be

$$w(t) = \begin{pmatrix} \cos(\alpha_d(t)) \\ \sin(\alpha_d(t)) \end{pmatrix} \quad (4)$$

Then, in vector forms

$$d(t) = w^T(t)\theta^*, \quad u(t) = w^T(t)\theta(t) \quad (5)$$

and

$$\begin{aligned} y(t) &= P(s)[u(t) - d(t)] \\ &= P(s)[w^T(t)(\theta(t) - \theta^*)] \end{aligned} \quad (6)$$

The notation $P(s)[(\cdot)]$ denotes the time-domain output of the LTI system $P(s)$ with input (\cdot) . (6) falls into the framework of standard adaptive control theory [2] [9], and various algorithms are available to update the adaptive parameters.

Fig. 4 shows the block diagram representation of the AFC algorithm with augmented error, where $w(t)$ is the regressor

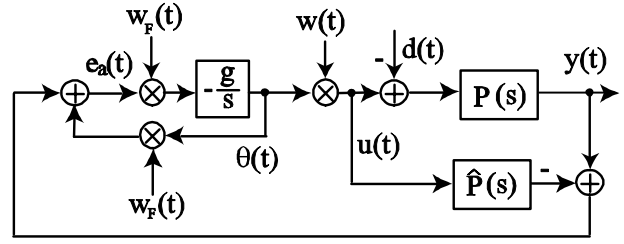


Fig. 4. Generalized block diagram of AFC with augmented error algorithm

vector defined in (4), and $w_F(t)$ is the filtered regressor vector defined as

$$w_F(t) = \hat{P}(s)[w(t)] \quad (7)$$

$\hat{P}(s)$ is the estimate of the plant $P(s)$. The adaptive parameters are updated by

$$\begin{aligned} \dot{\theta}(t) &= -g w_F(t) e_a(t) \\ e_a(t) &= y(t) + w_F^T(t)\theta(t) - \hat{P}(s)[u(t)] \end{aligned} \quad (8)$$

where $g > 0$ is the adaptation gain. The control signal is obtained as

$$u(t) = w^T(t)\theta(t) \quad (9)$$

Normally, the plant $P(s)$ is assumed to be stable, *i.e.*, it has no right half plane poles. If not, a stabilizing controller should be used and the AFC algorithm should be applied to the closed-loop system.

Under the condition that $\hat{P}(s) = P(s)$, the augmented error becomes

$$\begin{aligned} e_a(t) &= y(t) + w_F^T(t)\theta(t) - \hat{P}(s)[u(t)] \\ &= w_F^T(t)(\theta(t) - \theta^*) \end{aligned}$$

Letting the parameter error vector $\phi(t) = \theta(t) - \theta^*$, the system is then described by

$$\begin{aligned} \dot{\phi}(t) &= \dot{\theta}(t) = -g w_F(t) e_a(t) \\ &= -g w_F(t) w_F^T(t) \phi(t) \end{aligned} \quad (10)$$

The adaptive algorithm with augmented error is known to be stable from the result below.

Lemma 1: Let $w(t)$ be a piecewise continuous vector function of time. The system described by the differential equation

$$\dot{\phi}(t) = -g w(t) w^T(t) \phi(t)$$

is Lyapunov stable and all trajectories are bounded with

$$\|\phi(t)\| \leq \|\phi(0)\|$$

If $w(t)$ is *persistently exciting* (PE), the equilibrium point $\phi(t) = 0$ is globally exponentially stable.

Proof of the lemma can be found in [9], pp. 73–74 .

For the AE algorithm, w is replaced by w_F , and therefore, w_F must be PE to ensure the convergence of $\theta(t)$ to θ^* . If the frequency is constant, the PE condition requires that both the frequency of the disturbance and the frequency response of the plant at the frequency of the disturbance

be nonzero. The application of the above lemma is based on the assumption that the plant estimate is exact. If the plant estimate $\hat{P}(s)$ is not the same as the true plant $P(s)$, the AFC using AE algorithm has nevertheless good robustness to plant uncertainties as will be shown in simulations.

III. MODELLING OF A SINUSOIDAL DISTURBANCE WITH TIME-VARYING FREQUENCY AND IMP COMPENSATOR

An appropriate model for a disturbance of the form (1) is

$$\begin{aligned}\dot{x}(t) &= A_d(t)x(t) \\ d(t) &= C_d x(t)\end{aligned}\quad (11)$$

where

$$\begin{aligned}A_d(t) &= \begin{bmatrix} 0 & \omega_d(t) \\ -\omega_d(t) & 0 \end{bmatrix} \\ C_d(t) &= \begin{bmatrix} 0 & 1 \end{bmatrix}\end{aligned}\quad (12)$$

The state transition matrix associated with $A_d(t)$ is

$$\Phi(t, \tau) = \begin{bmatrix} \cos \int_{\tau}^t \omega_d(\lambda) d\lambda & \sin \int_{\tau}^t \omega_d(\lambda) d\lambda \\ -\sin \int_{\tau}^t \omega_d(\lambda) d\lambda & \cos \int_{\tau}^t \omega_d(\lambda) d\lambda \end{bmatrix}$$

Therefore, the disturbance in (1) is the solution of the nonautonomous system in (11) with initial conditions

$$x(0) = \begin{bmatrix} -\theta_s^* \\ \theta_c^* \end{bmatrix}$$

Note that the state-space realization used in [5]

$$\begin{aligned}\dot{x}(t) &= \begin{bmatrix} 0 & 1 \\ -\omega_d^2(t) & 0 \end{bmatrix} x(t) \\ d(t) &= \begin{bmatrix} 0 & 1 \end{bmatrix} x(t)\end{aligned}\quad (13)$$

is *not* appropriate as a model of the disturbance $d(t)$ in (1). This implementation only works well if the frequency is constant or slowly varying. For a rapidly varying frequency $\omega_d(t)$, the model should be changed to (12) or adjusted to be [4]

$$\dot{x}(t) = \begin{bmatrix} 0 & 1 \\ -\omega_d^2(t) & \frac{\dot{\omega}_d(t)}{\omega_d(t)} \end{bmatrix} x(t)\quad (14)$$

To design an IMP controller, one starts the controller with an internal model of the disturbance

$$\begin{aligned}\dot{x}_c(t) &= A_d(t)x_c(t) + z(t) \\ u(t) &= \begin{bmatrix} 0 & 1 \end{bmatrix} x_c(t)\end{aligned}\quad (15)$$

where $A_d(t)$ is given in (12), $u(t)$ is the controller output, and $z(t)$ is a signal obtained by a separate module of the controller, which is designed to ensure a stable closed-loop system. The parameter ω_d appears linearly in (12), so that an LPV design technique can be used. Although not immediately obvious, several AFC algorithms [4] associated with disturbances of varying frequencies are exactly equivalent to *linear time-varying* (LTV) compensators including the disturbance model. This equivalence is shown to hold for an algorithm with augmented error in the next section.

IV. EQUIVALENCE BETWEEN AFC ALGORITHM WITH AE AND LTV COMPENSATOR

Theorem 1: The adaptive system with AE algorithm in Fig. 4 is equivalent to the LTV system shown in Fig. 5 with

$$\begin{aligned}A_c(t) &= A_d(t) - gB(t)B^T(t) \\ B_c(t) &= -gB(t) \\ C_c(t) &= \begin{bmatrix} 0 & 1 \end{bmatrix}\end{aligned}\quad (16)$$

where

$$\begin{aligned}B(t) &= R(t)w_F(t) \\ R(t) &= \begin{bmatrix} \sin(\alpha_d(t)) & -\cos(\alpha_d(t)) \\ \cos(\alpha_d(t)) & \sin(\alpha_d(t)) \end{bmatrix}\end{aligned}\quad (17)$$

and $A_d(t)$ is defined in (12).

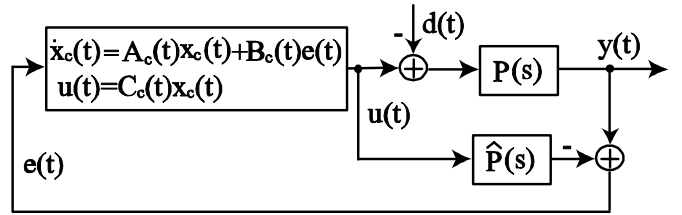


Fig. 5. LTV equivalence for the augmented error algorithm

Proof: the plant output can be represented as

$$y(t) = P(s) [u(t) - d(t)]$$

Define a linear transformation $R(t)$ such that $x_c(t) = R(t)\theta(t)$, then

$$\begin{aligned}\dot{x}_c(t) &= \dot{R}(t)\theta(t) + R(t)\dot{\theta}(t) \\ &= \dot{R}(t)R^{-1}(t)x_c(t) - gR(t)w_F(t)e_a(t) \\ &= A_d(t)x_c(t) - gB(t)e_a(t) \\ &= A_c(t)x_c(t) + v(t)\end{aligned}$$

where

$$v(t) = -gB(t) \left(y(t) - \hat{P}(s)[u(t)] \right)$$

This result can be checked by noting that

$$\begin{aligned}\dot{R}(t) &= \omega_d(t) \begin{bmatrix} \cos \alpha_d(t) & \sin(\alpha_d(t)) \\ -\sin(\alpha_d(t)) & \cos(\alpha_d(t)) \end{bmatrix} \\ R^{-1}(t) &= R^T(t) \\ \dot{R}(t)R^{-1}(t) &= A_d(t)\end{aligned}$$

with $R(t)$ and $B(t)$ defined in (17).

The control signal is

$$\begin{aligned}u(t) &= w^T(t)\theta(t) = w^T R^{-1}(t)x_c(t) \\ &= \begin{bmatrix} 0 & 1 \end{bmatrix} x_c(t)\end{aligned}$$

Since the determinant of $R(t)$ is always equal to 1, the linear transformation between $x_c(t)$ and $\theta(t)$ and its inverse are well-defined for all $t \geq 0$. Thus, the two systems are equivalent. \square

Notice that the equivalent controller includes the disturbance model defined in (11) (12), for the disturbance with time-varying frequency.

Let

$$\begin{aligned}\tilde{x}_c(t) &= x_c(t) - x_{ss}(t) \\ \tilde{u}(t) &= u(t) - d(t)\end{aligned}$$

where $x_{ss}(t)$ is the steady state of $x_c(t)$. We now show a result that applies when the plant model is exact.

Theorem 2: If the plant estimate $\hat{P}(s) = P(s)$, then the system in Fig. 5 is equivalent to the system in Fig. 6.

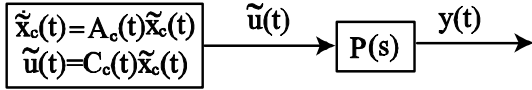


Fig. 6. LTV equivalence for exact plant estimate

Proof: inspired by the disturbance model in Section III, if

$$d(t) = \theta_c^* \cos(\alpha_d(t)) + \theta_s^* \sin(\alpha_d(t))$$

the signal $x_{ss}(t)$ can be defined as

$$\begin{aligned}x_{ss}(t) &= \begin{bmatrix} -\theta_s^* \cos(\alpha_d(t)) + \theta_c^* \sin(\alpha_d(t)) \\ d \end{bmatrix} \\ &= R(t)\theta^*\end{aligned}$$

Thus

$$\begin{aligned}\frac{d\tilde{x}_c(t)}{dt} &= A_c(t)x_c(t) + gB(t)P(s)[d] \\ &\quad - \dot{R}(t)R^{-1}(t)x_{ss}(t) \\ &= A_c(t)\tilde{x}_c(t) + gB(t)P(s)[d] \\ &\quad - gB(t)B^T(t)x_{ss}(t)\end{aligned}$$

and

$$\begin{aligned}B^T(t)x_{ss}(t) &= w_F^T(t)R^T(t)R(t)\theta^* \\ &= (\hat{P}(s)[w])^T\theta^* = \hat{P}(s)[w^T\theta^*] \\ &= \hat{P}(s)[d]\end{aligned}$$

Since $\hat{P}(s) = P(s)$, the result is apparent by letting $\tilde{u}(t) = u(t) - d(t)$. \square

If $\hat{P}(s) = P(s)$, the AE system shown in Fig. 4 is also equivalent to the system in Fig. 7, which is shown in (10). Note that the state-space representation Fig. 7 is also equivalent to the LTV system in Fig. 6 by using the linear transformation $\tilde{x}_c(t) = R(t)\phi(t)$.

V. SIMULATION RESULTS

In this section of simulation results, we consider the linear two-mass-spring-damper system of [6], which is illustrated in Fig. 8. $d(t)$ is the external sinusoidal disturbance force acting on the second mass, and the output of the system is the acceleration of the second mass. In [6], the control signal acts on the first mass, and we consider that case later. First, we will consider the case where the control signal (force)

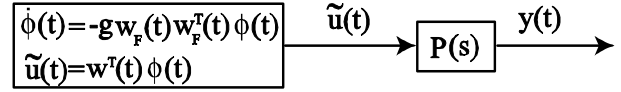


Fig. 7. Alternative LTV equivalence for exact plant estimate

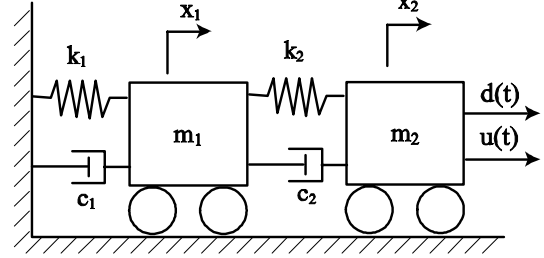


Fig. 8. Two-mass-spring-damper system

acts on the second mass, *i.e.* the sinusoidal disturbance and the control signal are at the same location.

The parameters are selected to be the same as in [6] where $m_1 = m_2 = 1$, $k_1 = k_2 = 100$, $c_1 = c_2 = 1$. Then, the corresponding plant in Fig. 4 is

$$P(s) = \frac{s^2(s^2 + 2s + 200)}{(s^2 + 0.382s + 38.2)(s^2 + 2.618s + 261.8)} \quad (18)$$

The disturbance $d(t)$ has a time-varying frequency changing between 3 rad/s and 33 rad/s. The disturbance $d(t)$ and its corresponding time-varying frequency $\omega_d(t)$ are shown in Fig. 9. The open-loop plant output (*i.e.*, without any compensation) is shown in Fig. 10.

In order to demonstrate the advantage of the augmented error algorithm over the pseudo-gradient algorithm of [4], a comparative simulation was done by setting all the initial conditions to zero and the adaptation gain to $g = 100$. The plant output for both cases are shown in Fig. 11. From the figure, one can see that the pseudo-gradient algorithm makes the system unstable even though the open-loop system is stable. With the augmented error algorithm, the output of the system converges to zero. The instability of the pseudo-

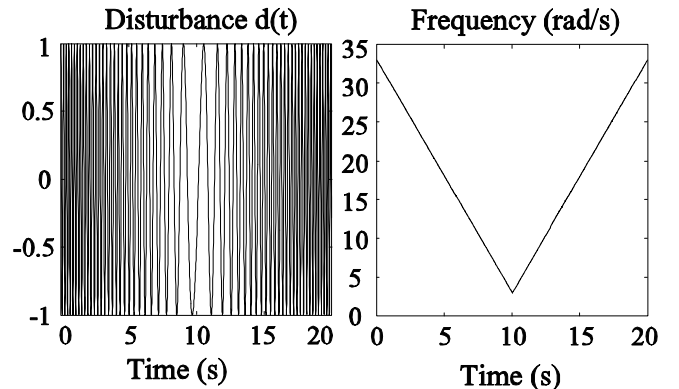


Fig. 9. Sinusoidal disturbance (left) and its time-varying frequency(right)

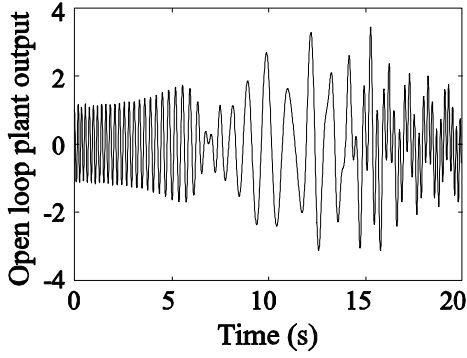


Fig. 10. Plant output without any compensation

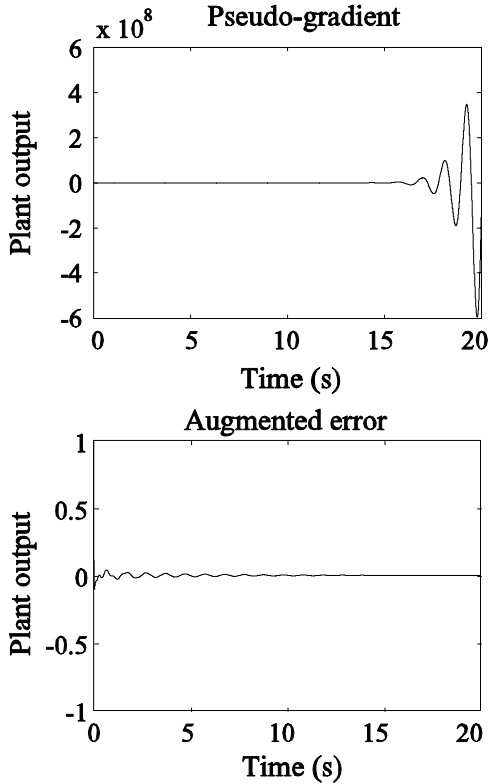


Fig. 11. AFC scheme with: pseudo-gradient algorithm (top) and augmented error algorithm (bottom)

gradient algorithm can be expected since $P(s)$ is not strictly positive real (SPR). However, the augmented error algorithm ensures stability without SPR conditions on the plant.

Next, simulations are used to evaluate the robustness of the augmented error algorithm based on nonaccurate plant estimates. Assume that

$$\hat{P}(s) = \frac{\sigma}{s + \sigma} P(s)$$

where $\sigma > 0$. Simulation results are shown in Fig. 12 for various values of σ . Good performance can be obtained if σ is large enough ($\sigma \geq 100$), which can be seen from the cases where $\sigma = 1000$ and $\sigma = 100$.

Finally, we show how the AE algorithm can be extended,

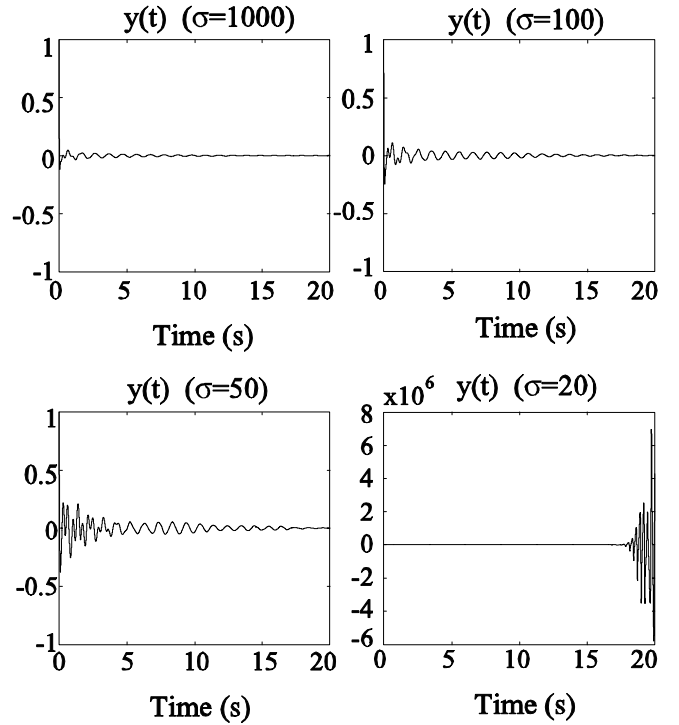


Fig. 12. Robustness of augmented error algorithm for different σ

at least approximately, to the case where the disturbance does not act at the same location as the control input. In particular, instead of acting on the second mass in Fig. 8, the control signal now acts on the first mass. The AE algorithm can be applied to the system as shown in Fig. 13, by adding a filter $\hat{P}_2^{-1}(s)$ to cancel the effect of $P_2(s)$. Then, the output of the AE algorithm is $\bar{u}(t)$ and the estimated plant model used in the AE algorithm is still $\hat{P}(s)$.

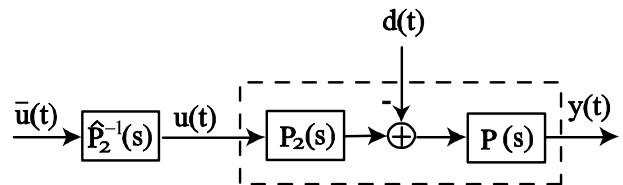


Fig. 13. Controller structure when $d(t)$ and $u(t)$ act at different locations

In this example, $P_2(s)$ is

$$P_2(s) = \frac{s + 100}{s^2 + 2s + 200}$$

Since $P_2(s)$ is strictly proper, $P_2^{-1}(s)$ is not proper. In order to implement the controller, we approximate $\hat{P}_2^{-1}(s)$ in Fig. 13 by

$$\hat{P}_2^{-1}(s) = \frac{1000}{s + 1000} P_2^{-1}(s)$$

The plant output obtained from a simulation is shown in Fig. 14. One sees that the plant output is greatly suppressed by comparing the open-loop output in Fig. 10. The residual

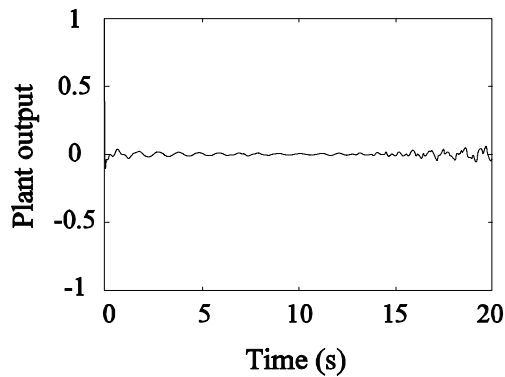


Fig. 14. Plant output for control signal acting on first mass with augmented error

output of the AE algorithm is also much lower than the results shown in [6].

VI. CONCLUSIONS

An adaptive feedforward cancellation scheme using an augmented error algorithm has been described to reject a sinusoidal disturbance with time-varying frequency. Slow frequency variation was not assumed. The control law has been shown to be equivalent to a linear time-varying compensator incorporating the internal model principle. Performance was validated by simulations, and it was shown that the

scheme exhibited good robustness to plant uncertainties. An advantage of the approach is that the design of a stable compensator can easily be achieved, as long as the plant is stable and sufficiently well known.

REFERENCES

- [1] A. Alleyne & M. Tharayil, "Semi-active internal model control for passive disturbance rejection," *Proc. of the American Control Conference*, pp. 1438–1443, 2001.
- [2] K. J. Åström & B. Wittenmark, *Adaptive Control*, 2nd ed., Addison-Wesley, 1995.
- [3] G. Bengtsson, "Output regulation and internal models—a frequency domain approach," *Automatica*, vol. 13, pp. 333–345, 1977.
- [4] M. Bodson, "Equivalence between adaptive cancellation algorithms and linear time-varying compensators," *Proc. of IEEE Conf. Decision Contr.*, pp. 638–643, 2004.
- [5] L. J. Brown & Q. Zhang, "Periodic disturbance cancellation with uncertain frequency," *Automatica*, vol. 40, no. 4, pp. 631–637, 2004.
- [6] H. Du, L. Zhang, Z. Lu & X. Shi, "LPV technique for the rejection of sinusoidal disturbance with time-varying frequency," *IEE Proc.-Control Theory Appl.*, vol. 150, no. 2, pp. 132–138, 2003.
- [7] B. A. Francis & W. M. Wonham, "The internal model principle of control theory," *Automatica*, vol. 12, pp. 457–465, 1976.
- [8] R.V. Monopoli, "Model reference adaptive control with an augmented error signal," *IEEE Trans. on Automatic Control*, vol. 19, pp. 474–484, 1974.
- [9] S. Sastry & M. Bodson, *Adaptive control: stability, convergence, and robustness*, Prentice-Hall: Englewood Cliffs, NJ, 1989.
- [10] C. C. de Wit and L. Praly, "Adaptive eccentricity compensation," *IEEE Trans. on Control Systems Technology*, vol. 8, no. 5, pp. 757–766, 2000.
- [11] Y. Xu, M. de Mathelin, & D. Knittel, "Adaptive rejection of quasi-periodic tension disturbances in the unwinding of a non-circular roll," *Proc. of the American Control Conference*, pp. 4009–4014, 2002.